Received: 9 May 2019 | Revised: 17 September 2019 | Accepted: 11 October 2019

DOI: 10.1002/jlcr.3814

RESEARCH ARTICLE

WILEY Journal of Labelled Compounds and Radiopharmaceuticals

Synthesis, radiosynthesis, and positron emission tomography neuroimaging using 5-[^{18}F]fluoro-L-amino suberate

Santosh R. Alluri[1] | Kathinka E. Pitman[1,2] | Eirik Malinen[1,2] | Patrick J. Riss[1,2,3]

[1] Realomics Strategic Research Initiative (SRI), Department of Chemistry, University of Oslo, Oslo, Norway

[2] Realomics Strategic Research Initiative (SRI), Department of Physics, University of Oslo, Oslo, Norway

[3] Realomics Strategic Research Initiative (SRI), NMS AS, Oslo, Norway

Correspondence
Patrick J. Riss, Realomics Strategic Research Initiative (SRI), Department of Chemistry, University of Oslo, Oslo, Norway.
Email: patrick.riss@kjemi.uio.no

Funding information
Faculty of Mathematics and Natural Sciences, University of Oslo

System xc- (Sx_c-) has emerged as a new biological target for PET studies to detect oxidative and excitotoxic stress. Notably, applications have, thus far, been limited to tumour imaging although Sx_c^-) may play a major role in neurodegeneration. The synthesis procedures of tosylate precursor and its translation to Sx_c- PET tracer 5[18F]fluoro-L-amino suberate by manual and automated radiosyntheses are described. A brain-PET study has been conducted to evaluate the tracer uptake into brain in healthy mice.

KEYWORDS
System x_c, brain imaging, mouse, radiosynthesis

1 | INTRODUCTION

System x_c^- (Sx_c^-) is an antiporter that facilitates L-cystine import and L-glutamate export across the cell plasma membrane. The intracellular cystine reduces into cysteine, which is the synthetic precursor to the glutathione (GSH) biosynthetic pathway. The latter serves as an oxidative protection agent in cells by scavenging reactive oxygen species (ROS).[1-3] Bannai and Kitamura were the first to describe a carrier system that promotes sodium-independent L-cystine or L-glutamate uptake into cultured human fibroblasts.[4] Structurally, Sx_c^- belongs to heterodimeric amino acid transporters and consists of a heavy subunit (4F2hc) and a light subunit (xCT). The latter is substrate specific and allows the binding and transport of amino acids across the plasma membrane.[1] Sx_c^- expression is observed in a variety of tissues such as brain, kidney, liver, ovary, breast, and various other cell types.[3] Functional studies on Sx_c^- indicate that Sx_c^- activity is mainly governed by the transcriptional regulation of its xCT subunit.[5] Experimental shreds of evidence strongly suggest that the xCT expression is regulated by amino acid deprivation (for example cystine) and oxidative stress. Up-regulation of xCT mRNA in response to oxidative stress has been assessed in various tumors.[3,6-8]

The expression and function of Sx_c^- in the central nervous system (CNS) is also well studied.[1] Firstly, GSH makes the Sx_c^- role significant in the brain. The brain regions are known to consume high levels of oxygen and have limited antioxidant capacity to suppress ROS generated by various processes. GSH production and maintenance is indispensable to prevent oxidative dam-

age in the brain.[9] Secondly, the amount of extracellular glutamate produced via Sx_c^- export during stressful insults to tissue (hypoxia; low oxygen supply) or other pathological environments is significant within the brain.[1,3] This is because glutamate is an essential neurotransmitter and its transport via Sx_c^- is a nonvesicular route. It can thus improve the brain function via neuronal signalling, or its excess efflux can lead to excitotoxicity mediated neuronal diseases. Correspondingly, Sx_c^- activity was assessed in Multiple sclerosis disease state in the CNS using (S)-4-(3-[^{18}F]Fluoropropyl)-L-glutamic acid ([^{18}F]FSPG)-PET.[10-12] We were also interested in positron emission tomography (PET) imaging of Sx_c^- in the brain, which could provide an insight into glutamate-mediated excitotoxicity occurring as part of neurodegenerative cascades, for example after stroke.

L-Glutamate and L-cystine are specific substrates to Sx_c^-. Glutamate analogs with varying carbon chain length, for example, 2-amino adipate, 2-amino pimelate, 2-amino suberate (Asu), and their fluorinated analogs, were also explored as substrates/inhibitors to Sx_c^-.[6,8] Herein, we describe the synthesis, manual and automated radiosynthesis of 5-[^{18}F]fluoro-L-amino suberate ([^{18}F]FASu) and preclinical PET in mice using [^{18}F]FASu to evaluate brain uptake of [^{18}F]FASu.

2 | RESULTS AND DISCUSSION

2.1 | Organic chemistry

The synthesis of FASu **1** is shown in Scheme 1. The syntheses were carried out using reported methods[6,13,14] with some modifications. In brief, commercially available, functional group protected L-glutamate **2** was used as a starting material. At first, the carboxylic acid **2** was methylated using methyl chloroformate under basic reaction conditions to obtain **3.** Then the methyl ester was reduced by DIBAL-H to the aldehyde derivative **5**. Subsequently, the aldehyde of **5** was coupled to a 3-carbon length *tert*-butyl propiolate in presence of LDA to provide the overall 8-carbon skeleton **6** in a moderate yield. Here, the compound **6** was obtained as diastereomeric mixture (NMR). The diastereomeric mixture was inseparable in chromatography

(silica gel column or reversed phase high-performance liquid chromatography [RP-HPLC]). Therefore, it was used as such and preceded further. The alkyne bond of compound **6** was hydrogenated with H_2 and Pd/C to prepare **7**. The –OH group of **7** was then converted to its –tosyl derivative **8,** which is a precursor for ^{18}F-radiolabeling. TBAF $(t\text{BuOH})_4$[14] was used as fluoride source to achieve fluorinated intermediate **9** in good yield**.** Then finally, compound **1** was obtained upon the acidic hydrolysis of **9.** The –Boc protective groups were chosen provided the simple deprotection conditions and stable under the basic ^{18}F-radiolabeling reaction conditions. Scheme 2 shows the radiosynthesis of [^{18}F]FASu.

2.2 | Radiochemistry

At first, the radiolabelling step[16] and the hydrolysis conditions were optimized manually to obtain useful yields of the final [^{18}F]**1** (Table 1).

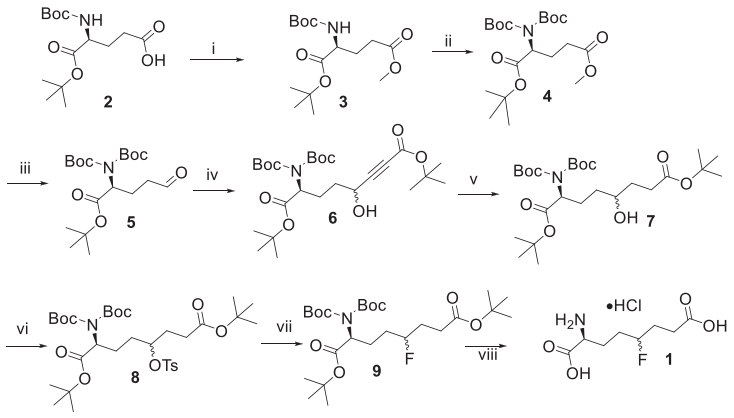

SCHEME 1 Synthesis of [^{18}F]FASu precursor 8 and FASu 1; *Reagents and conditions*; i. DCM, 0°C, Et_3N, DMAP, methyl chloroformate, rt, 2 h, **3** 93%; ii. CH_3CN, rt, $(Boc)_2O$, 24 h, **4** 90%; iii. THF, −78°C, DIBAL-H, 1 h, water, **5** 60%; iv. *tert*-Butyl propiolate, THF, −78°C, lithium diisopropylethylamine, 30 min, then **5,** 2 h, **6** 50%; v. EtOAc, rt, Pd/C, H_2, 4 h, **7** 93%; vi. DCM, 0°C, Et_3N, pyridine, DMAP, $(Ts)_2O$, rt, 24 h, **8** 80%; vii. CH_3CN, rt, TBAF $(t\text{BuOH})_4$, 70°C, 30 min, **9** 63%; viii. Ethereal HCl, rt, 24 h, **1** 95%

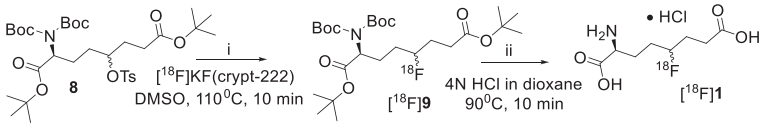

SCHEME 2 Synthesis of [^{18}F]**9**, [^{18}F]FASu ([^{18}F]**1**); *Reagents and conditions*; i. ~4 mg **8,** ^{18}F (2-4 GBq), 1.8 mg K_2CO_3, 11 mg crypt-222, C_{18} cartridge or preparative HPLC purification; ii. 0.5 mL 4N HCl in dioxane, tC_{18} cartridge purification

TABLE 1 Radio-TLC conversion of **8** to [^{18}F]**1**[a] ($n \geq 5$)

Entry	Temperature, °C/time, min	TLC conversion[b], ±5%
1	80/10	61
2	80/20	60
3	100/10	76
4	110/10	90
5	110/20	85
6	120/10	84
7[c]	90/10	60
8[d]	110/10	48

[a]Labellings reactions were performed with ^{18}F (1-5 GBq), **8** (3-4 mg), K_2CO_3 (1.8 mg), crypt-222 (11 mg), and DMSO (0.5 mL).

[b]25% EtOAc in hexanes.

[c]In CH_3CN.

[d]In DMF.

The conditions (Table 1, entry 4) DMSO, 110 °C and 10 minute reaction time were found superior compared with other conditions. The manual synthetic procedures were repeated ($n = 15$) for reproducibility and then automated for multiple productions of [^{18}F]FASu.

2.3 | [^{18}F]FASu automation

The no-carrier added (nca) two-step radiosynthesis of [^{18}F]FASu was automated in a hot cell equipped with a Scintomics HBIII synthesis module. Before proceeding to the automated production, a test sequence comprising of valves, dispensers, vacuum, nitrogen pressure, reaction vials, heaters, radioactivity detectors, cartridges, and HPLC equipment was arranged as shown in Figure 1.

The test sequence was then added to the programmable controller of the module to allow the visualization of all the processes on the computer. QMA-seppak cartridges were preactivated with 10 mL water followed by 10 mL air. The C_{18}, tC_{18} SPE cartridges were preactivated with 5 mL CH_3CN followed by 5 mL water.

Table 2 shows the comparison of decay corrected, isolated radiochemical yields of manual and automated syntheses of [^{18}F]FASu from the end of bombardment (see experimental).

2.4 | PET imaging

Formulated [^{18}F]FASu was used in a pilot study to test if a sufficient amount of the radiotracer reaches the healthy brain to allow for PET imaging. Animal protocols were approved by the National Animal Research Authority and adhered to the guidelines of the Federation of European Laboratory Animal Science Association (FELASA). Two mice were placed within the field of view of a Siemens microPET Focus 120 small animal PET camera

TABLE 2 Decay corrected, radioactivity yield of [^{18}F]FASu in manual (n = 15), and automated syntheses (n = 20)

Step	Radioactivity Yield of the Manual Synthesis, ±4%/time, min	Radioactivity Yield of the Automated Synthesis, ±3 %/time, min
1	20/60	19/60
2	51/30	45/30
Overall	10/90	9/90

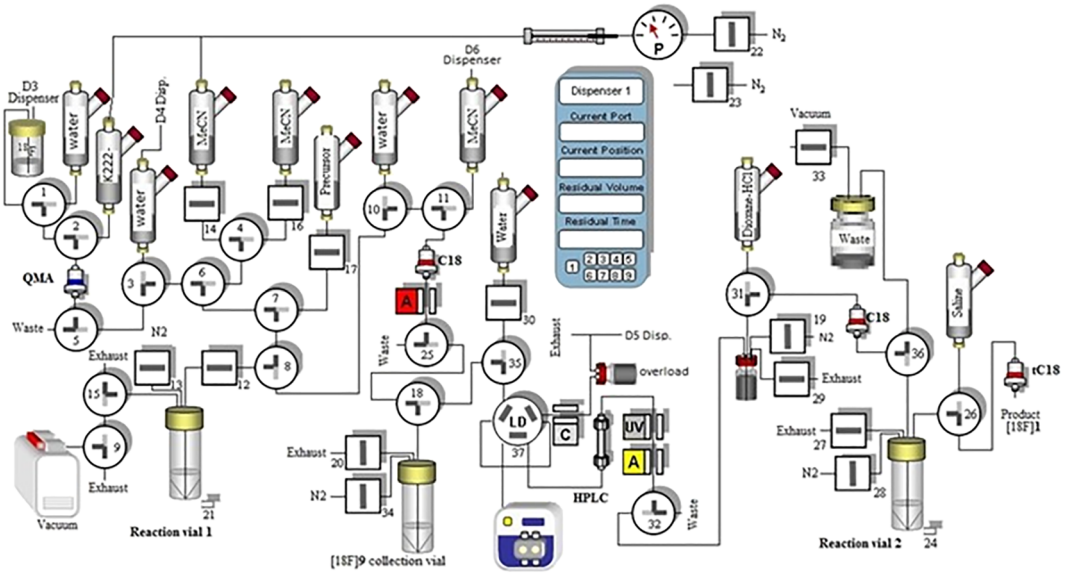

FIGURE 1 Schematic of components of [^{18}F]FASu automation

under mild isoflurane anaesthesia (1.5%) and ~5 MBq of [^{18}F]FASu in 0.9% NaCl was administered via the tail vein at the start of a 30 minute recording session.

PET data were reconstructed using an OSEM3D-MAP algorithm to give a dynamic sequence of 17 frames with time resolution 10-300 seconds and voxel size of 0.87×0.87×0.80 mm^3, and then analysed using Pmod3.8 software. Following visual inspection of summed images covering the first seven frames of the recording, volumes of interest (2.5-3.85 mm diameter) were placed in the brain and left kidney of the animals and time activity curves were extracted.[17] Figure 2 shows a summed image of the first seven frames (0-1 min) and averaged time activity curves for blood, brain and kidney over 30 minutes.

As evident from both image and time activity traces, the retention of [^{18}F]FASu in the healthy brain is not very pronounced. Peak concentrations of up to 1.6%ID/mL (percent injected dose per millilitre) were reached within 1 minute, followed by slow washout over the remainder of the data recording. See Figure 2 results.

Blood-to-brain radioactivity concentration ratios improve in favour of brain over time from an initial 177:1 to about 8:1 in the late frames. We assume that there is some specific retention possibly related to inward transport of the radioligand into cells rather than binding which causes the appearance of the curve. When attempting kinetic modelling of the data using the one tissue compartment and two tissue compartment models (1TCM and 2TCM, respectively) with whole blood activity as the input.[18] we obtained a fairly good fit for 1TCM. The rate constant for extraction of the tracer into brain (K_1) was 0.0013±0.0009mL/cm^{3}s^{-1}. While the fit for 2TCM was not plausible, setting rate constant k_4 to 0 produced a somewhat better result. This implies an irreversible component in the brain uptake of the tracer such as inward transport, which explains the slower clearance of the tracer from brain relative to blood and thus supports brain penetration. Considering the high endogeneous concentration of cysteine, L-glutamate and other substrates of the transporter in brain which will compete for the binding site with [^{18}F]FASu, the observation of binding becomes unlikely. These consideration lead us to assume that [^{18}F]FASu shows limited uptake into brain, some specific retention due to inward transport and low background. This may support further characterization of the radiotracer in models of oxidative stress in brain.

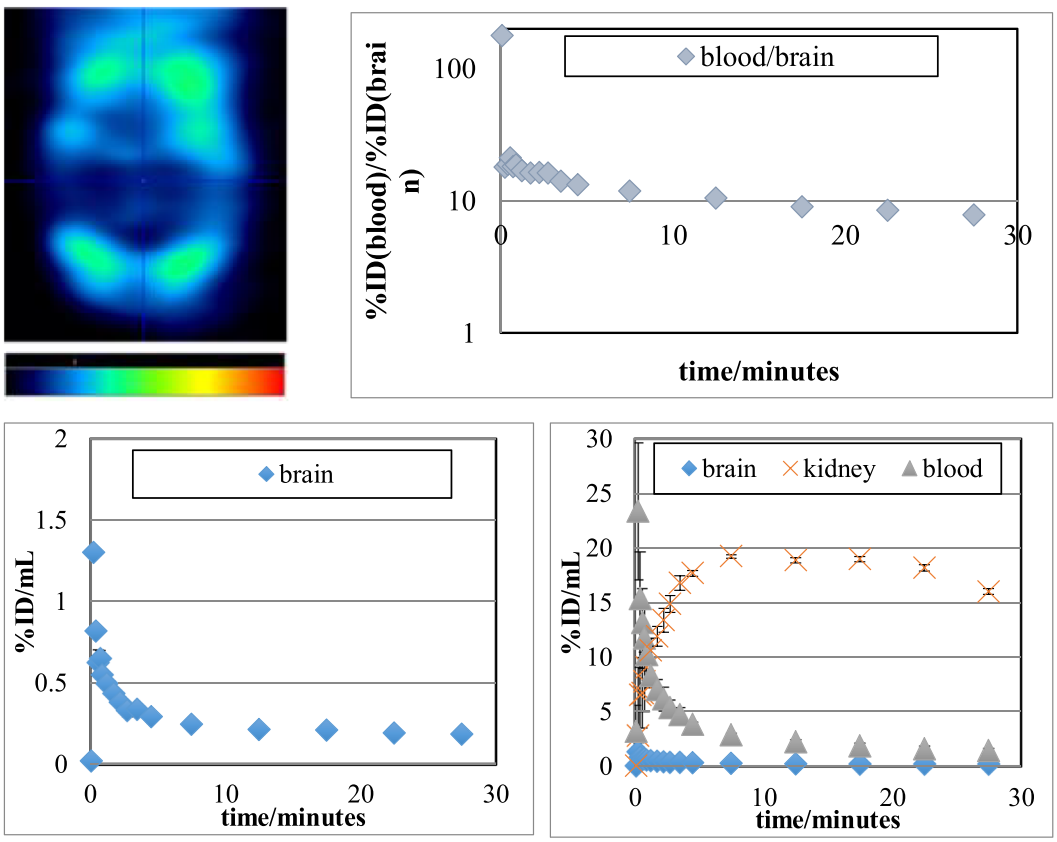

FIGURE 2 A summed PET image of first seven frames (left), blood-to-brain concentration ratios (top right) and dynamic PET data for brain (bottom left), blood, brain and kidney (bottom right)

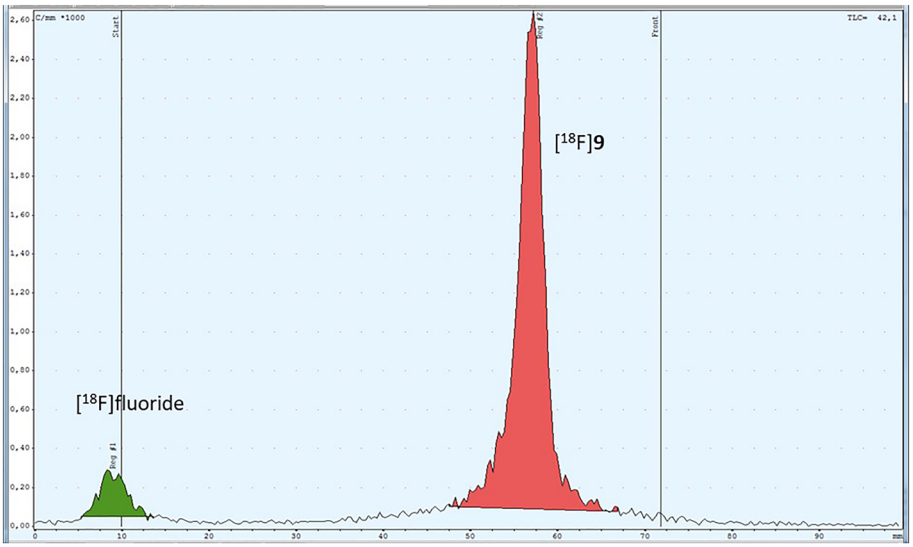

FIGURE 3 Radio-TLC of reaction crude after labelling; ~4 mg **8,** ^{18}F (2-4 GBq), 1.8 mg K_2CO_3, 11 mg crypt-222, DMSO (0.5 mL), 110 ^{0}C, 10 min, TLC condition- 25% EtOAc in hexanes

3 | CONCLUSION

[^{18}F]FASu was produced in a fully automated process with 9±3% yield over 90 minutes. Small animal imaging revealed some brain uptake and very low specific accumulation in healthy brain, which bodes well for neuroimaging in rodent models.

4 | EXPERIMENTAL

4.1 | General information

All the reactions were carried out in oven-dried glassware under an atmosphere of nitrogen or argon. All commercially obtained reactants and reagents were used as such without any further purification. Hexanes were distilled prior to use. Anhydrous THF, dichloromethane were purchased from Sigma Aldrich (Norway). For lower temperature reactions, ice bath (0°C) and acetone-dry ice bath (−78°C) were used. Reactions were monitored by TLC using silica gel coated aluminium plates with F-254 indicator. The corresponding reaction products were visualized by $KMnO_4$ staining (1.5 g $KMnO_4$, 10 g K_2CO_3, 0.2 g NaOH in 100 mL H_2O). ^{1}H (400 MHz), ^{13}C (101 MHz), ^{19}F (376 MHz) NMR were recorded on Bruker AVI 400 instrument. High resolution ESI mass spectra were recorded with a TOF quadruple Micromass QTOF 2 W instrument. Radio-TLCs were analysed using a raytest miniGita radioTLC scanner (Raytest GmBH, Straubenhardt, Germany). All other radioactivity measurements during labelling experiments were performed using a Wallac Wizard well counter (PerkinElmer, Oslo, Norway). Radio-UV HPLC analyses were performed on Agilent 1200 analytical system equipped with UV detector, Raytest GmBH radioactivity detector. In analytical HPLC system, Supelco HSF5 column (250 × 4.6 mm, 5 μm), wavelength 220 nm are used.

4.2 | Organic syntheses

4.2.1 | 1-(tert-butyl) 5-methyl-2-(*tert*-butoxycarbonyl)-L-glutamate (3)[6]

Et_3N (0.350 mL, 2.472 mmol), DMAP (0.024 g, 0.164 mmol) and methyl chloroformate (0.153 mL, 0.197 mmol) were added to a solution of compound $_2$ (0.500 g, 1.648 mmol) in anhydrous DCM (10 mL) at 0°C. The whole reaction mixture was warmed to room temperature and stirred for 90 minutes. It was then quenched with cold water (10 mL) and extracted with DCM (2x 15 mL). The combined organic layers were dried (Na_2SO_4), concentrated, and the crude was purified by column chromatography (0-35% EtOAc in hexanes). Product was colourless oil, which became white solid upon storage at −20°C. R_f: 0.68 (35% EtOAc in hexanes); Yield 0.486 g, 1.534 mmol, 93%; ^{1}H NMR (400 MHz, Chloroform-*d*) δ 5.07 (d, J = 8.2 Hz, 1H), 4.19 (q, J = 7.4 Hz, 1H), 3.67 (s, 3H), 2.38 (td, J = 8.9, 6.5 Hz, 2H), 2.14 (dq, J = 14.0, 6.7, 6.3 Hz, 1H), 1.98-1.86 (m, 1H), 1.45 (d, 18H); ^{13}C NMR (101 MHz, $CDCl_3$) δ 173.7, 171.6, 155.7, 82.6, 80.1, 53.8, 52.1, 30.5, 28.7, 28.4; HRESI-MS (*m*/*z*) calcd for $C_{15}H_{27}NO_6Na$ $[M+Na]^+$ 340.1838; found 340.1731

4.2.2 | 1-(tert-butyl) 5-methyl-2-(bis-(*tert*-butoxycarbonyl)-L-glutamate (4)

DMAP (0.035 g, 0.254 mmol) and compound $_3$ (0.538 g, 1.696 mmol) were dissolved in CH3CN (3 mL). (Boc)2O (1.000 g, 5.089 mmol) in CH3CN (2 mL) was added at room temperature and the mixture was stirred for 24 hours. The pink solution was concentrated and loaded as such onto silica gel column and purified by 0 to 20% EtOAc in hexanes. Product was colourless oil. R_f: 0.51 (20% EtOAc in hexanes). Yield 0.636 g, 1.527 mmol, 90%; ^{1}H NMR (400 MHz, Chloroform-*d*) δ 4.84-4.72 (m, 1H), 3.66 (s, 3H), 2.46-2.32 (m, 3H), 2.22-2.17 (m, 1H), 1.47 (d, 27H); ^{13}C NMR (101 MHz, $CDCl_3$) δ 172.9, 168.9, 152.0, 82.6, 81.1, 57.9, 51.3, 30.6, 27.7, 27.7, 24.4; HRESI-MS (*m*/*z*) calcd for $C_{20}H_{35}NO_8Na$ $[M+Na]^+$ 440.2363; found 440.2254

4.2.3 | (*S*)-2-[Bis-(*tert*-butoxycarbonylamino)]-4-(formylbutanoic acid)-*tert*-butyl ester (5)

1M solution of DIBAL-H (2.108 mmol) in hexane was added over 5 minutes to a solution of compound $_4$ (0.800 g, 1.918 mmol) in anhydrous diethyl ether (12 mL) at -78°C and the obtained mixture was stirred for 1 hour at same temperature. Following this time, reaction was quenched with 0.2 mL water and warmed to room temperature after which the white precipitate was filtered through short celite column using EtOAc eluent. The crude solution was concentrated and purified by column chromatography (0-40% EtOAc in hexanes). Product was colourless oil. R_f: 0.38 (20% EtOAc in hexanes), 0.445 g, 1.151 mmol, yield 60%; ^{1}H NMR (400 MHz, $CDCl_3$) δ 9.78 (t, 1H), 4.77-4.73 (m, 1H), 2.63-2.37 (m, 3H), 2.21-2.11 (m, 1H), 1.52 (s, 18H), 1.46 (s, 9H); ^{13}C NMR (101 MHz, $CDCl_3$) δ 201.3, 169.2, 152.3, 83.1, 81.3, 58.1, 40.7, 28.0, 27.9, 21.9; HRESI-MS (*m*/*z*) calcd for $C_{19}H_{30}NO_7Na$ $[M+Na]^+$ 410.2257; found 410.2150

4.2.4 | (2*S*)-di-*tert*-butyl 2-((bis-*tert*-butoxycarbonyl)amino)-5-hydroxyoct-6-ynedioate (6)

1M THF solution of lithium diisopropylamine (0.500 mmol) was slowly added to *tert*-butyl propiolate (0.080 mL, 0.482 mmol) dissolved in anhydrous THF (2 mL) at −78°C and stirred for 30 minutes after which compound **5** (0.170 g, 0.439 mmol) in THF (1.5 mL) was added and stirring continued for 2 hours at same temperature. The reaction was then quenched with 1M NH_4Cl (5 mL) and warmed to room temperature and extracted with EtOAc (3x 10 mL). The combined organic layers were dried (Na_2SO_4), concentrated and the crude was purified by column chromatography (0-30% EtOAc in hexanes) R_f; 0.55 (30% EtOAc in hexanes). The product was colourless oil and yield 0.112 g, 0.220 mmol, 50% which obtained as a diastereomeric mixture as judged by NMR; ^{1}H NMR (400 MHz, $CDCl_3$) δ 4.79-4.73 (m, 1H), 4.55-4.49 (m, 1H), 2.36-2.01 (m, 4H), 1.52 (s, 18 H), 1.48 (s, 9H), 1.46 (s, 9H); ^{13}C NMR (101 MHz, $CDCl_3$) δ 170.07, 169.95, 152.93, 152.85, 152.75, 85.30, 85.26, 84.11, 83.55, 83.49, 81.94, 81.92, 77.79, 77.68, 77.48, 77.16, 62.43, 61.90, 58.92, 58.76, 34.14, 28.49, 28.43, 28.40, 25.59, 25.18; HRESI-MS (*m*/*z*) calcd for $C_{26}H_{43}NO_9Na$ $[M+Na]^+$ 536.2938; found 536.2825

4.2.5 | (2*S*)-di-*tert*-butyl 2-((bis-*tert*-butoxycarbonyl)amino)-5-hydroxyoctanedioate (7)

Pd/C (0.194 mmol) was added to a solution of compound $_6$ (0.240 g, 0.467 mmol) in EtOAc (5 mL) and the mixture was flushed with nitrogen for 5 minutes followed by H_2 for 30 minutes. The reaction was then stirred for 4 hours under H_2 balloon. Following this time, Pd was filtered off and the crude was concentrated to obtain **7** as colourless oil (diastereomeric mixture), which was used as such in next step. R_f: 0.50 (30% EtOAc in hexanes). Yield 0.225 g, 0.435 mmol, 93%; ^{1}H NMR (400 MHz, $CDCl_3$) δ 4.73-4.59 (m, 1H), 3.58-3.53 (m, 1H), 2.29-1.98 (m, 2H), 1.90-1.56 (m, 6H), 1.50-1.43 (d, 36 H); ^{13}C NMR (101 MHz, $CDCl_3$) δ 173.57, 173.54, 169.99, 169.73, 152.57, 152.47, 82.85, 82.82, 81.27, 81.24, 80.42, 80.40, 77.22, 77.01, 76.79, 71.22, 70.68, 58.92, 58.69, 34.40, 34.18, 32.31, 32.22, 32.16, 32.06, 28.08, 28.03, 27.94, 25.71, 25.57; HRESI-MS (*m*/*z*) calcd for $C_{26}H_{47}NO_9Na$ $[M+Na]^+$ 540.3251; found 540.3138

4.2.6 | (2*S*)-Di-*tert*-butyl 2-((bis-*tert*-butoxycarbonyl)amino)-5-(tosyloxy) octanedioate (8)

Et_3N (0.212 mmol) and pyridine (0.212 mmol) was added sequentially to the compound **7** (0.055 g, 0.106 mmol) dissolved in dry DCM (2 mL) at 0°C and stirred for 10 which was followed by the addition of DMAP (0.011 mmol) and toluene sulfonic anhydride (0.233 mmol) as solid under N_2. The whole reaction was stirred for 16 hours at room temperature, and the pink solution was quenched with water (3 mL) extracted with DCM (2x 10 mL). The organic layers were dried (Na_2SO_4), concentrated, and the crude was purified by column chromatography (0-

30% EtOAc in hexanes) to obtain **8** as colourless oil (diastereomeric mixture). R_f: 0.45 (20% EtOAc in hexanes). Yield 0.057 g, 0.085 mmol, 80%; ^{1}H NMR (400 MHz, Chloroform-*d*) δ 7.79 (dd, J = 8.4, 2.1 Hz, 2H), 7.36-7.28 (m, 2H), 4.70-4.53 (m, 2H), 2.43 (s, 3H), 2.29-2.16 (m, 2H), 1.99-1.50 m, 6H), 1.53-1.39 (m, 36H); ^{13}C NMR (101 MHz, $CDCl_3$) δ 172.26, 169.73, 169.70, 152.79, 145.00, 134.81, 134.74, 130.28, 130.26, 128.21, 128.18, 83.38, 83.35, 82.65, 82.47, 81.79, 81.75, 80.94, 77.80, 77.68, 77.48, 77.16, 59.07, 58.77, 31.75, 31.54, 31.18, 31.08, 29.80, 29.44, 28.53, 28.50, 28.48, 28.40, 25.08, 24.81, 22.10; HRESI-MS (m/z) calcd for $C_{33}H_{53}NO_{11}SNa$ $[M+Na]^+$ 694.3339; found: 694.3244

4.2.7 | (2*S*)-di-*tert*-butyl 2-((bis-*tert*-butoxycarbonyl)amino)-5-fluorooctanedioate (9)

TBAF (tBuOH)$_4$ (0.024 g, 0.044 mmol) was added to the compound **8** (0.015 g, 0.022 mmol) dissolved in anhydrous CH_3CN (1 mL) at room temperature and heated to 70°C for 30 minutes. Following this time, the reaction was quenched with water and extracted with EtOAc (2x 5 mL). The crude was purified by column chromatography (0-15% EtOAc in hexanes) to obtain **9** as a colourless oil (diastereomeric mixture). Yield 0.007 g, 0.014 mmol, 63%; ^{1}H NMR (400 MHz, Chloroform-*d*) δ 4.79-4.40 (m, 2H), 2.44-1.56 (m, 8H), 1.52-1.42 (m, 36H); ^{13}C NMR (101 MHz, $CDCl_3$) δ 172.81, 170.00 (d, J_{CF} = 7.86 Hz), 152.90 (d, J_{CF} = 2.36 Hz), 152.81, 93.40 (dd, J_{CF} = 168.85 Hz, 24.51 Hz), 83.34 (d, J_{CF} = 2.24 Hz), 81.77 (d, J_{CF} = 1.77 Hz), 81.73, 81.67, 81.54, 80.84, 80.58, 80.52, 80.44, 59.25, 59.07 (t, J_{CF} = 7.40 Hz), 58.86, 35.88, 32.59, 32.37 (d, J_{CF} = 3.17 Hz), 31.60 (m), 31.05, 30.88, 30.58 (d, J_{CF} = 18.16 Hz), 28.62, 28.58, 28.55, 28.52, 28.49, 28.42, 25.50, 25.44 (d, J_{CF} = 3.51 Hz); ^{19}F NMR ($CDCl_3$, 564 MHz) δ 183.60-183.25 (m,) −182.90 to −182.50 (m); ESI-MS $C_{26}H_{46}NO_{18}FNa$ $[M+Na]^+$ 542.3, calcd 542.3

4.2.8 | (*2S*)-2-amino-5-fluorooctanedioic acid. HCl salt (1)

5M aq. HCl (1.5 mL) was added to the compound **9** (0.008 g, 0.015 mmol) dissolved in ether (1.5 mL) at room temperature and stirred vigorously for 24 hours. The crude was freeze dried to obtain **1** as white solid in quantitative yield. 0.004 g, 0.015 mmol; ^{1}H NMR (400 MHz, D_2O) δ 4.09-3.92 (m, 2H), 2.48-2.23 (m, 2H), 1.96-1.32 (m, 8H); ^{13}C NMR (101 MHz, D_2O) δ 179.16, 179.0, 177.98, 172.44, 94.79, 94.74, 93.16, 93.10, 53.00, 52.95, 29.56, 29.52, 29.45, 27.63, 27.60, 27.10, 25.74, 25.69; ESI-MS $C_{18}H_{15}NO_4F$ [M+H]+: 208.1, calcd 208.1

4.3 | Radiochemical synthesis

4.3.1 | Manual synthesis

Step 1: Aqueous ^{18}F produced by ^{18}O[p, n]^{18}F nuclear reaction was trapped on QMA cartridge (Waters corporation) and eluted with 0.5 mL of K_2CO_3: 4,7,13,16,21,24-Hexaoxa-1,10-diazabicyclo[8.8.8]hexacosane (crypt-222) (1.4 mg: 10.9 mg in 400 μL CH_3CN and 100 μL water) in a 4 mL v-vial. The residual water was azeotropically dried with acetonitrile (3x 1 mL) at 85°C under nitrogen stream. To the dried [^{18}F]KF-crypt-222 complex was added ~4 mg of **8** dissolved in 0.5 mL DMSO at room temperature under nitrogen atmosphere. The vial was closed and stirred for 10 minutes at 110°C and cooled to room temperature. The reaction was quenched with 4 mL water and passed through a C_{18} cartridge (preactivated with 5 mL CH_3CN and 5 mL water). The cartridge was rinsed further with 2x 6 mL water. The radioactive intermediate was eluted with 1 mL anhydrous acetonitrile in a reverse flow. The acetonitrile content was further passed through a silica cartridge and acetonitrile was dried under nitrogen stream at 85°C for 5 minutes. Purity of the product was monitored by analytical HPLC using Supelco HSF5 C_{18} column (250 × 4.6 mm, 5 μm) with mobile phase consisting of 65% CH_3CN, 35% water at a flow rate of 1 mL/minute in an isocratic elution mode. The product can also be purified by semipreparative HPLC system as mentioned in automation protocol. Both the manual and HPLC purifications gave the radiochemical purity of [^{18}F]**9** more than 98% (Figure 4). The decay corrected yield at the end of step 1 is 20±4% in time of 60 minutes from end of bombardment.

Step 2: About 0.5 mL of 4N HCl in dioxane was added to the dried [^{18}F]**9** and stirred at 90°C for 10 minutes in a closed vial. Following this time, dioxane was evaporated under N_2 stream; the reaction contents were cooled, diluted with 1 mL water and carefully neutralized to pH 7 with 4N aq. NaOH, and then passed through a tC_{18} cartridge in a 2 mL vial and formulated in 0.9% saline and then passed through a 0.22-μm filter for further studies. About 5 μL of the final product was injected into analytical HPLC for quality control using analytical Supelco C_{18} HSF5 column (Figure 5). Decay corrected radiochemical yield of [^{18}F]**1** from [^{18}F]**9** is 51±4%. The overall decay corrected radiochemical yield 10±4% in total reaction time of 90 minutes.

4.3.2 | Automation protocol

The total synthesis time is approximately 90 minutes starting from trapping ^{18}F onto QMA until formulation

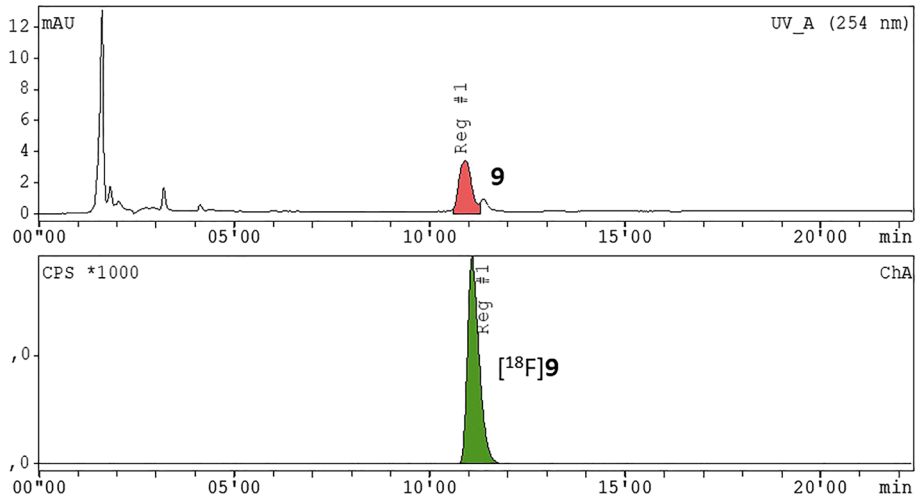

FIGURE 4 Radio-HPLC trace of purified [^{18}F]**9** and co-injected with **9,** Supelco HSF5 C_{18} column (250 × 4.6 mm, 5 μm), 65%CH_3CN; 35% H_2O, isocratic, 1 mL/min

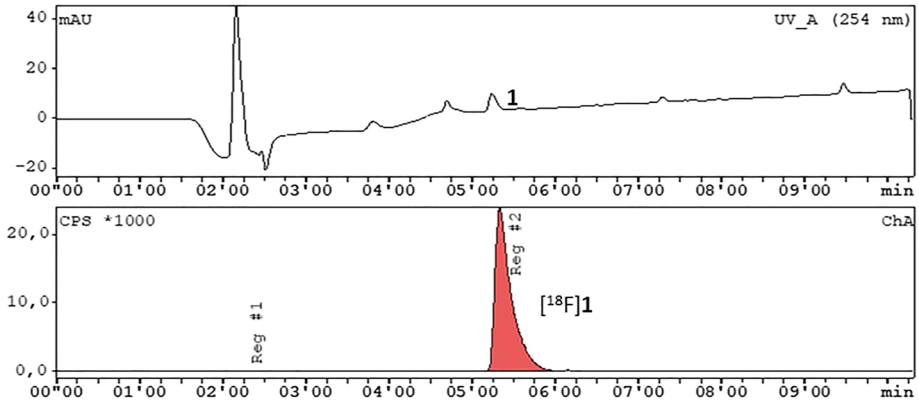

FIGURE 5 Radio-HPLC trace of [^{18}F]**1,** co-injected with **1** Supelco HSF5 C_{18} column (250 × 4.6 mm, 5 μm), 0.1% TFA in H_2O (A), 0.1% TFA in CH_3CN (B); *Gradient (*1 mL/min*)* 0 minutes- 99.5% A, 15 minutes 20% A, 30 minutes 99.5% A

of [^{18}F]**1**. The automated production was initiated (time *t* = 0 minutes) with the nca ^{18}F (25 GBq) in $H_2{}^{18}O$ (2.4 mL) placing inside the hot cell (D3) (see Figure 1). The nca ^{18}F was passed through a preactivated QMA- seppak (Waters AS, Norway) through valves 1 and 2 and the ^{18}O enriched water recovered in a waste recovery vial. The QMA trapped ^{18}F was then washed with 1 mL of water through valve 1 and 2 followed by eluting with 0.6 mL K_2CO3/ crypt222 mixture (1.8 mg K_2CO_3/0.1 mL H_2O: 11 mg crypt-222/0.5 mL CH_3CN) through valve 2 into a reaction vial 1. Azeotrpoic drying of ^{18}F-potassium-cryptate complex in vial 1 was performed under reduced pressure (200 mbar) at 90°C with two rounds of 0.5 mL CH_3CN dispensing through valves 4 and 6. The content of the reaction vessel 1 was frequently purged with nitrogen to minimize the reflux and to ensure good mixing of the content. Following this time, vessel 1 temperature was increased to 110°C and the precursor **8** (~4 mg in 0.5 mL anhydrous DMSO) dispensed through valve 17 into the reaction vial 1. At this point, all the valves are closed and the reaction continued for 10 minutes at 110°C and then the vial 1 was cooled to ambient temperature in a stream of compressed air.

The vial 1 content was diluted with water (3 mL) dispensed through valve 10 and passed through C_{18} cartridge through valve 8. The C_{18} trapped product was eluted into collection vial using 1 mL CH_3CN (D6) and diluted with water (3 mL) through valve 30. This solution was injected into semipreparative HPLC system equipped with semiprep HSF5 C_{18} column (5 μm, 250 × 10 mm), mobile phase (65% CH_3CN-35% H_2O) and flow rate (4 mL/min). The desired [^{18}F]**9** was collected between 11 and 13 minutes into a 50-mL collection flask. The collected HPLC fractions were passed through a preactivated C_{18}-seppak cartridge through valve 31 to remove excess water and CH_3CN into the waste. The C_{18} trapped [^{18}F] **9** was then eluted using 4N HCl (0.5 mL) in dioxane dispensed through valve 31 into the reaction vial 2 (3.2

GBq). At this point, vial 2 temperature increased to 90°C and all the valves are closed and the reaction continued for 10 minutes at 90°C. The vial 2 was then evacuated under reduced pressure and nitrogen flow to remove excess dioxane and acid content. Following this time, vessel 2 was cooled to room temperature under a stream of compressed air and diluted with saline (1 mL) dispensed through valve 26. This solution was passed through valve 26 through a preactivated tC_{18} cartridge into a collection vial (1.8 GBq) to obtain [^{18}F]**1**. The saline solution of [^{18}F]**1** was taken out of the hot cell in a lead container and passed through a 0.22 μm filter to remove the solid traces.

ACKNOWLEDGEMENTS

Funding from Faculty of Mathematics and Natural Sciences, University of Oslo was gratefully acknowledged (Patrick Riss).

FUNDING INFORMATION

System x_c^- (Sx_c^-) has emerged as a new biological target for positron emission tomography (PET) studies to detect oxidative and excitotoxic stress. Notably, applications have, thus far, been limited to tumour imaging although Sx_c^- may play a major role in neurodegeneration. The synthesis procedures of tosylate precursor and its translation to Sx_c^- PET tracer 5-[^{18}F]fluoro-L-amino suberate by manual and automated radiosyntheses are described. A brain-PET study has been conducted to evaluate the tracer uptake into brain in healthy mice.

ORCID

Patrick J. Riss https://orcid.org/0000-0002-3887-7065

REFERENCES

1. Bridges RJ, Natale NR, Patel SA. System xc cystine/glutamate antiporter: an update on molecular pharmacology and roles within the CNS. *Br J Pharmacol.* 2012;165(1):20-34.
2. Lo M, Wang YZ, Gout PW. The x(c)- cystine/glutamate antiporter: a potential target for therapy of cancer and other diseases. *J Cell Physiol.* 2008;215(3):593-602.
3. Lewerenz J, Hewett SJ, Huang Y, et al. *Antioxid Redox Signal.* 2013;18:522-555.
4. Bannai S, Kitamura E. *J Biol Chem.* 1979;265:2372-2376.
5. Habib E, Linher-Melville K, Lin HX, Singh G. Expression of xCT and activity of system xc(-) are regulated by NRF2 in human breast cancer cells in response to oxidative stress. *Redox Biol.* 2015;5:33-42.
6. Webster JM, Morton CA, Johnson BF, et al. *J Nucl Med.* 2014;55:657-664.
7. Baek S, Mueller A, Lim Y-S, et al. (4S)-4-(3-18F-fluoropropyl)-L-glutamate for imaging of xC transporter activity in hepatocellular carcinoma using PET: preclinical and exploratory clinical studies. *J Nucl Med.* 2013;54(1):117-123.
8. Koglin N, Mueller A, Berndt M, et al. *Clin Cancer Res.* 2011;17:6000-6011.
9. Valdovinos-Flores C, Gonsebatt ME. The role of amino acid transporters in GSH synthesis in the blood-brain barrier and central nervous system. *Neurochem Int.* 2012;61(3):405-414.
10. Hoehne A, James ML, Alam IS, et al. *J Neuroinflammation.* 2018;15:55.
11. Martín A, Vázquez-Villoldo N, Gómez-Vallejo V, et al. In vivo imaging of system xc- as a novel approach to monitor multiple sclerosis. *Eur J Nucl Med Mol Imaging.* 2016;43(6):1124-1138.
12. Domercq M, Szczupak B, Gejo J, et al. *Martín A.* 2016;6:10-14.
13. Yang H, Jenni S, Colovic M, et al. ¹⁸F-5-Fluoroaminosuberic Acid as a Potential Tracer to Gauge Oxidative Stress in Breast Cancer Models. *J Nucl Med.* 2017;58(3):367-373.
14. Alluri SR, Riss PJ. Stereospecific radiosynthesis of 3-fluoro amino acids: access to enantiomerically pure radioligands for positron emission tomography. *Org Biomol Chem.* 2018;16(13):2219-2224. https://doi.org/10.1039/C8OB00184G.
15. Kim DW, Jeong HJ, Lim ST, Sohn MH. *Angew Chemie - Int Ed.* 2008;47:8404-8406.
16. Riss PJ, Rösch F. A convenient chemo-enzymatic synthesis and 18F-labelling of both enantiomers oftrans-1-toluenesulfonyloxymethyl-2-fluoromethyl-cyclopropane. *Org Biomol Chem.* 2008;6(24):4567-4574. https://doi.org/10.1039/b812777h.
17. Pitman KE, Alluri SR, Kristian A, et al. Influx rate of 18F-fluoroaminosubericacid reflects cystine/glutamate antiporter expression in tumour xenografts. *Eur J Nucl MedMol Imaging.* 2019;46(10):2190-2198. https://doi.org/10.1007/s00259-019-04375-8.here.
18. Riss PJ, Hong YT, Williamson D, et al. Validation and quantification of [18F]altanserin binding in the rat brain using blood inputand reference tissue modeling. *J Cereb BloodFlow Metab.* 2011;31(12):2334-2342. https://doi.org/10.1038/jcbfm.2011.94.

SUPPORTING INFORMATION

Additional supporting information may be found online in the Supporting Information section at the end of the article.

How to cite this article: Alluri SR, Pitman KE, Malinen E, Riss PJ. Synthesis, radiosynthesis, and positron emission tomography neuroimaging using 5-[^{18}F]fluoro-L-amino suberate. *J Label Compd Radiopharm*. 2020;63:6–14. https://doi.org/10.1002/jlcr.3814